




Remeshing-Free Graph-based Finite Element Method for Fracture Simulation: Supplement

A. Mandal¹  and P. Chaudhuri²  and S. Chaudhuri¹ 

¹ Department of Electrical Engineering, Indian Institute of Technology Bombay, India
{avirupmandal, sc}@ee.iitb.ac.in

² Department of Computer Science and Engineering, Indian Institute of Technology Bombay, India
{paragc}@cse.iitb.ac.in

1. Derivation of Internal Elastic Forces along the Edges

As introduced in Section 3.2 of the main paper, the internal elastic force for graph-based FEM can be written as

$$\mathbf{f}_{e_i}^{int} = V_e \frac{\partial \Psi^e}{\partial \mathbf{r}_i^e} = 2V_e \sum_{\substack{j=1 \\ j \neq i}}^{n_e} \frac{\partial \Psi^e}{\partial (d_{ij}^e)^2} d_{ij}^e \hat{\mathbf{d}}_{ij}^e \quad (1)$$

where \mathbf{r}_i^e is the world position vector for node i of element Δ_e . The parameter $d_{ij}^e = \|\mathbf{r}_i^e - \mathbf{r}_j^e\|$ denotes the distance between the i^{th} and j^{th} nodes of Δ_e and $\hat{\mathbf{d}}_{ij}^e$ is unit vector along d_{ij}^e . Moreover, V_e and n_e represent the volume and the number of nodes of Δ_e respectively. Here we give the full derivation of the above equation.

$$\begin{aligned} \mathbf{f}_{e_i}^{int} &= V_e \frac{\partial \Psi^e}{\partial \mathbf{r}_i^e} \\ &= V_e \sum_{\substack{j=1 \\ j \neq i}}^{n_e} \frac{\partial \Psi^e}{\partial (d_{ij}^e)^2} \frac{\partial (d_{ij}^e)^2}{\partial \mathbf{r}_i^e} \quad (\text{Using chain rule of differentiation}) \\ &= V_e \sum_{\substack{j=1 \\ j \neq i}}^{n_e} \frac{\partial \Psi^e}{\partial (d_{ij}^e)^2} \frac{\partial d_{ij}^e}{\partial \mathbf{r}_i^e} 2d_{ij}^e \\ &= V_e \sum_{\substack{j=1 \\ j \neq i}}^{n_e} \frac{\partial \Psi^e}{\partial (d_{ij}^e)^2} \frac{\partial \sqrt{(\mathbf{r}_i^e - \mathbf{r}_j^e)^T (\mathbf{r}_i^e - \mathbf{r}_j^e)}}{\partial \mathbf{r}_i^e} 2d_{ij}^e \\ &= V_e \sum_{\substack{j=1 \\ j \neq i}}^{n_e} \frac{\partial \Psi^e}{\partial (d_{ij}^e)^2} \frac{1}{2\sqrt{(\mathbf{r}_i^e - \mathbf{r}_j^e)^T (\mathbf{r}_i^e - \mathbf{r}_j^e)}} \frac{\partial [(\mathbf{r}_i^e - \mathbf{r}_j^e)^T (\mathbf{r}_i^e - \mathbf{r}_j^e)]}{\partial \mathbf{r}_i^e} 2d_{ij}^e \\ &= V_e \sum_{\substack{j=1 \\ j \neq i}}^{n_e} \frac{\partial \Psi^e}{\partial (d_{ij}^e)^2} \frac{1}{2d_{ij}^e} \frac{\partial [(\mathbf{r}_i^e)^T \mathbf{r}_i^e - (\mathbf{r}_i^e)^T \mathbf{r}_j^e - (\mathbf{r}_j^e)^T \mathbf{r}_i^e + (\mathbf{r}_j^e)^T \mathbf{r}_j^e]}{\partial \mathbf{r}_i^e} 2d_{ij}^e \end{aligned}$$

This is the author's version of the work. It is posted here for your personal use. Not for redistribution. The definitive Version of Record was published in Computer Graphics Forum, <https://doi.org/10.1111/cgf.14725>.

$$\begin{aligned}
&= V_e \sum_{\substack{j=1 \\ j \neq i}}^{n_e} \frac{\partial \Psi^e}{\partial (d_{ij}^e)^2} \frac{\partial \left[(\mathbf{r}_i^e)^T \mathbf{r}_i^e - 2(\mathbf{r}_i^e)^T \mathbf{r}_j^e + (\mathbf{r}_j^e)^T \mathbf{r}_j^e \right]}{\partial \mathbf{r}_i^e} \quad (\text{As } (\mathbf{r}_i^e)^T \mathbf{r}_j^e = (\mathbf{r}_j^e)^T \mathbf{r}_i^e, \text{ both being scalar values}) \\
&= V_e \sum_{\substack{j=1 \\ j \neq i}}^{n_e} \frac{\partial \Psi^e}{\partial (d_{ij}^e)^2} 2(\mathbf{r}_i^e - \mathbf{r}_j^e) \\
&= 2V_e \sum_{\substack{j=1 \\ j \neq i}}^{n_e} \frac{\partial \Psi^e}{\partial (d_{ij}^e)^2} d_{ij}^e \hat{\mathbf{d}}_{ij}^e \tag{2}
\end{aligned}$$

2. Proof for Edge Length Dependence of Strain Energy Density

Theorem 2.1 Every element of the set of invariants $\mathbf{I}_V = \{I_C, II_C, III_C, IV_C, V_C\}$ can be expressed in closed form using only the length of the edges of a mesh used in FEM.

Proof Let us assume an element, Δ_e , of a mesh used in FEM in k -dimensional space, which consists of Z_l edges. Let τ_{ij} be the stretch ratio of an edge formed by nodes i and j of the same element,

$$\tau_{ij} = \frac{d_{ij}^e}{D_{ij}^e} \tag{3}$$

where d_{ij}^e and D_{ij}^e denote current and initial length of the edge respectively.

Now, projecting the Right Cauchy-Green deformation tensor \mathbf{C} along the edges, we can write,

$$\tau_{ij}^2 = \mathbf{C} \cdot (\mathbf{q}_{ij}^e \otimes \mathbf{q}_{ij}^e) = \mathbf{C} \cdot \mathbf{Q}_{ij}^e \tag{4}$$

where \otimes denotes tensor product and $\mathbf{Q}_{ij}^e \in \mathbb{R}^{k \times k}$. The projection vector, \mathbf{q}_{ij}^e , can be written in a k -dimensional space as

$$\mathbf{q}_{ij}^e = [\hat{\mathbf{d}}_{ij}^e \cdot \hat{\mathbf{i}}_1 \quad \hat{\mathbf{d}}_{ij}^e \cdot \hat{\mathbf{i}}_2 \quad \dots \quad \hat{\mathbf{d}}_{ij}^e \cdot \hat{\mathbf{i}}_k]^T$$

where $\{\hat{\mathbf{i}}_1, \hat{\mathbf{i}}_2, \dots, \hat{\mathbf{i}}_k\}$ denotes a set of orthogonal basis vectors of the k -dimensional space. Extending this formulation to all Z_l edges, we get

$$\mathcal{T} = \mathbf{C} \cdot \mathcal{Q} \tag{5}$$

where $\mathcal{T} \in \mathbb{R}^{Z_l}$ and $\mathcal{Q} \in \mathbb{R}^{k \times k \times Z_l}$, whose entries are equal to τ_{ij}^2 and \mathbf{Q}_{ij}^e respectively.

In order to express \mathbf{C} in terms of τ_{ij}^e we need to invert \mathcal{Q} , which is not always possible. However, we can determine \mathbf{C} as the solution to the following optimization problem

$$\mathbf{C} = \underset{\hat{\mathbf{C}}}{\operatorname{argmin}} \|\hat{\mathbf{C}} \cdot \mathcal{Q} - \mathcal{T}\|_2^2 \tag{6}$$

The solution to this optimization problem allows us to express \mathbf{C} in terms of \mathcal{T} and \mathcal{Q} .

The solution to the problem is given in closed form by

$$\hat{\mathbf{C}} = \mathcal{T} \cdot [\mathcal{Q} \otimes \mathcal{Q}]^\dagger \cdot \mathcal{Q} \tag{7}$$

where \dagger denotes pseudo-inverse.

It is evident from Equation 7 that Right Cauchy-Green deformation tensor, \mathbf{C} , is a function of the length of the edges, d_{ij}^e . Hence, so are all elements of \mathbf{I}_V and therefore, so is the hyper-elastic strain energy density, Ψ^e . \square

2.1. Discussion on the Proof

First let us write Equation 7 in summation notation for a 2D triangular element for more coherency. To do that first we will rewrite \mathcal{T} , \mathbf{C} and \mathbf{Q}_{ij}^e in vector format.

$$\begin{aligned}
\mathcal{T} &= [\mathcal{T}_1^2, \mathcal{T}_2^2, \mathcal{T}_3^2]^T \\
\mathbf{C} &= [\mathbf{c}_{xx}, \mathbf{c}_{yy}, \sqrt{2}\mathbf{c}_{xy}]^T \\
\mathbf{Q}_l &= [\mathbf{q}_{lx}^2, \mathbf{q}_{ly}^2, \sqrt{2}\mathbf{q}_{lx}\mathbf{q}_{ly}]^T \quad l \in Z_l \\
\mathcal{T}_l^2 &= \mathbf{C} \cdot \mathbf{Q}_l
\end{aligned} \tag{8}$$

where l denotes the set of three edges, Z_l , between nodes i and j . Similarly, the vectorized format \mathbf{Q}_{ij}^e is \mathbf{Q}_l . Following the same arguments as before the final expression can be written as

$$\begin{aligned} \mathbf{C} &= \underset{\hat{\mathbf{C}}}{\operatorname{argmin}} \sum_{l=1}^3 \|\hat{\mathbf{C}} \cdot \mathbf{Q}_l - \mathcal{T}_l^2\|_2^2 \\ \hat{\mathbf{C}} &= \sum_{l=1}^3 \mathcal{T}_l^2 \left[\sum_{l=1}^3 \mathbf{Q}_l \otimes \mathbf{Q}_l \right]^\dagger \mathbf{Q}_l \end{aligned} \quad (9)$$

In Equation 9 the quantity $\sum_{l=1}^3 \mathbf{Q}_l \otimes \mathbf{Q}_l$ is invertible only when the area/volume of a 2D/3D element is non-zero i.e. when it does not contain any degeneracy. In that case Equation 9 reduce to $\hat{\mathbf{C}} = \sum_{l=1}^3 \mathcal{T}_l^2 \mathbf{Q}_l^{-1}$ which is exactly equal to Equation 5 in matrix form. Thus, in such a scenario, the residual of Equation 7 goes to zero. On the other hand, when the form is not invertible for degenerate elements, $\hat{\mathbf{C}}$ becomes a close approximation of \mathbf{C} . However, in both cases, the final expression depends only on the edge lengths of the element.

3. Fractured Strain Energy Density: Linear Elasticity

3.1. Undamaged Condition

In linear elasticity the strain energy density for a tetrahedral element, Δ_e , can be written in terms of linear Cartesian strain $\boldsymbol{\varepsilon}_c^e$ and stress $\boldsymbol{\sigma}_c^e$ vectors as below.

$$\Psi^e = \frac{1}{2} \boldsymbol{\sigma}_c^e \cdot \boldsymbol{\varepsilon}_c^e = \frac{1}{2} \boldsymbol{\varepsilon}_c^e \mathbf{E} \cdot \boldsymbol{\varepsilon}_c^e \quad (10)$$

where $\boldsymbol{\sigma}_c^e = \boldsymbol{\varepsilon}_c^e \mathbf{E}$ and linear Cartesian strain $\boldsymbol{\varepsilon}_c^e = \frac{1}{2} (\mathbf{F} + \mathbf{F}^T) - \mathbf{I}$ is expressed in vector format (in Voigt notation).

$$\boldsymbol{\varepsilon}_c^e = [\varepsilon_{xx}^e \quad \varepsilon_{yy}^e \quad \varepsilon_{zz}^e \quad \varepsilon_{xy}^e \quad \varepsilon_{xz}^e \quad \varepsilon_{yz}^e] \quad (11)$$

The symmetric matrix \mathbf{E} denotes Young's modulus matrix [MG04].

For linear elasticity, the strain components along the edges can be written as

$$\varepsilon_{ij}^e = \frac{l_{ij}}{L_{ij}} \quad (12)$$

where L_{ij} and l_{ij} denote the original length and increase in length of the edge formed by nodes i and j . In vector format original length and increase in length can be expressed as below.

$$\begin{aligned} \mathbf{L}_d^e &= [L_{12}^e \quad L_{13}^e \quad L_{14}^e \quad L_{23}^e \quad L_{24}^e \quad L_{34}^e] \\ \mathbf{l}_d^e &= [l_{12}^e \quad l_{13}^e \quad l_{14}^e \quad l_{23}^e \quad l_{24}^e \quad l_{34}^e] \end{aligned} \quad (13)$$

For a tetrahedral element edge-based normal strain from Equation 12 can be written in matrix form as

$$\boldsymbol{\varepsilon}_d^e = [\varepsilon_{12}^e \quad \varepsilon_{13}^e \quad \varepsilon_{14}^e \quad \varepsilon_{23}^e \quad \varepsilon_{24}^e \quad \varepsilon_{34}^e] \quad (14)$$

For graph-based FEM we need to write down all the parameters e.g., strain energy density and internal force, using edge-based variables. Thus, transforming edge-based normal strain to Cartesian strain, Equation 10 can be rewritten as

$$\Psi^e = \frac{1}{2} \boldsymbol{\varepsilon}_c^e \mathbf{E} \cdot \boldsymbol{\varepsilon}_c^e = \frac{1}{2} [\mathbf{T}^{-1} [\boldsymbol{\varepsilon}_d^e]^T]^T \mathbf{E} \cdot [\mathbf{T}^{-1} [\boldsymbol{\varepsilon}_d^e]^T]^T \quad (15)$$

Now the nodal internal force vector \mathbf{f}_e^{int} of element Δ_e of volume V_e can be written as

$$\begin{aligned} \mathbf{f}_e^{int} &= V_e \frac{\partial \Psi^e}{\partial \mathbf{u}_e} = V_e \frac{\partial \Psi^e}{\partial \boldsymbol{\varepsilon}_c^e} \frac{\partial \boldsymbol{\varepsilon}_c^e}{\partial \mathbf{u}_e} = V_e \boldsymbol{\sigma}_c^e \frac{\partial \boldsymbol{\varepsilon}_c^e}{\partial \mathbf{u}_e} \\ &= V_e \boldsymbol{\sigma}_c^e \frac{\partial \boldsymbol{\varepsilon}_c^e}{\partial \mathbf{l}_d^e} \frac{\partial \mathbf{l}_d^e}{\partial \mathbf{u}_e} \quad (\text{Using Equation 13}) \\ &= V_e \boldsymbol{\sigma}_c^e \mathbf{A}_2^T \mathbf{A}_1^T = V_e \boldsymbol{\sigma}_c^e \mathbf{B} = V_e \boldsymbol{\varepsilon}_c^e \mathbf{E} \mathbf{B} \end{aligned} \quad (16)$$

where $\mathbf{A}_1 = \left[\frac{\partial \mathbf{l}_d^e}{\partial \mathbf{u}_e} \right]^T$, $\mathbf{A}_2 = \left[\frac{\partial \boldsymbol{\varepsilon}_c^e}{\partial \mathbf{l}_d^e} \right]^T$ and $\mathbf{B}^T = \mathbf{A}_1 \mathbf{A}_2$. The detailed expressions of \mathbf{A}_1 and \mathbf{A}_2 are given in the next section.

Similarly, we can formulate the tangent stiffness matrix in the graph-based FEM paradigm as below.

$$\begin{aligned}
\mathbf{k}_e &= \frac{\partial \mathbf{f}_e^{int}}{\partial \mathbf{u}_e} = V_e \left[\frac{\partial \boldsymbol{\varepsilon}_c^e}{\partial \mathbf{u}_e} \right]^T \left[\frac{\partial^2 \Psi^e}{\partial \boldsymbol{\varepsilon}_c^e \partial \boldsymbol{\varepsilon}_c^e} \right] \left[\frac{\partial \boldsymbol{\varepsilon}_c^e}{\partial \mathbf{u}_e} \right] \\
&= V_e \left[\frac{\partial \boldsymbol{\varepsilon}_c^e}{\partial \mathbf{l}_d^e} \frac{\partial \mathbf{l}_d^e}{\partial \mathbf{u}_e} \right]^T \mathbf{E} \left[\frac{\partial \boldsymbol{\varepsilon}_c^e}{\partial \mathbf{l}_d^e} \frac{\partial \mathbf{l}_d^e}{\partial \mathbf{u}_e} \right] \\
&= V_e \left[\frac{\partial \mathbf{l}_d^e}{\partial \mathbf{u}_e} \right]^T \left[\frac{\partial \boldsymbol{\varepsilon}_c^e}{\partial \mathbf{l}_d^e} \right]^T \mathbf{E} \left[\frac{\partial \boldsymbol{\varepsilon}_c^e}{\partial \mathbf{l}_d^e} \right] \left[\frac{\partial \mathbf{l}_d^e}{\partial \mathbf{u}_e} \right] \\
&= V_e \mathbf{A}_1 \mathbf{A}_2 \mathbf{E} \mathbf{A}_2^T \mathbf{A}_1^T = V_e \mathbf{B}^T \mathbf{E} \mathbf{B}
\end{aligned} \tag{17}$$

Note that both internal elastic force \mathbf{f}_e^{int} and tangent stiffness matrix \mathbf{k}_e match the formulation of conventional FEM.

3.2. Damaged Condition

When an element gets fractured the strain energy density from Equation 10 and Equation 15 can be written as

$$\begin{aligned}
\Psi^e &= \frac{1}{2} \boldsymbol{\sigma}_{c_{frac}}^e \cdot \boldsymbol{\varepsilon}_{c_{frac}}^e = \frac{1}{2} \boldsymbol{\varepsilon}_{c_{frac}}^e \mathbf{E} \cdot \boldsymbol{\varepsilon}_{c_{frac}}^e \\
\text{Using } [\boldsymbol{\sigma}_{c_{frac}}^e]^T &= \mathbf{T}^{-1} \boldsymbol{\zeta} \mathbf{T} [\boldsymbol{\sigma}_c^e]^T \text{ from main document} \\
&= \frac{1}{2} \left[\mathbf{T}^{-1} \boldsymbol{\zeta} \mathbf{T} [\boldsymbol{\varepsilon}_c^e]^T \right]^T \mathbf{E} \cdot \left[\mathbf{T}^{-1} \boldsymbol{\zeta} \mathbf{T} [\boldsymbol{\varepsilon}_c^e]^T \right]^T
\end{aligned} \tag{18}$$

Now following the same line of arguments as presented in Equation 16 and Equation 17, the internal force and tangent stiffness matrix for fractured elements can be represented as

$$\mathbf{f}_{e_{frac}}^{int} = V_e \boldsymbol{\varepsilon}_c^e \mathbf{T}^T \boldsymbol{\zeta} \mathbf{T}^{-T} \mathbf{E} \mathbf{T}^{-1} \boldsymbol{\zeta} \mathbf{T} \mathbf{B} \tag{19}$$

$$\mathbf{k}_{e_{frac}} = V_e \mathbf{B}^T \mathbf{T}^T \boldsymbol{\zeta} \mathbf{T}^{-T} \mathbf{E} \mathbf{T}^{-1} \boldsymbol{\zeta} \mathbf{T} \mathbf{B} \tag{20}$$

4. Full expressions for \mathbf{A}_1 and \mathbf{A}_2

Here we give the full expressions for \mathbf{A}_1 and \mathbf{A}_2 , from Equation 16 in the previous section.

4.1. Full expression of \mathbf{A}_1

$$\mathbf{A}_1 = \left[\frac{\partial \mathbf{l}_d^e}{\partial \mathbf{u}_e} \right]^T = \begin{bmatrix} \frac{\partial l_{12}^e}{\partial u_{1x}^e} & \frac{\partial l_{13}^e}{\partial u_{1x}^e} & \frac{\partial l_{14}^e}{\partial u_{1x}^e} & \frac{\partial l_{23}^e}{\partial u_{1x}^e} & \frac{\partial l_{24}^e}{\partial u_{1x}^e} & \frac{\partial l_{34}^e}{\partial u_{1x}^e} \\ \frac{\partial l_{12}^e}{\partial u_{1y}^e} & \frac{\partial l_{13}^e}{\partial u_{1y}^e} & \frac{\partial l_{14}^e}{\partial u_{1y}^e} & \frac{\partial l_{23}^e}{\partial u_{1y}^e} & \frac{\partial l_{24}^e}{\partial u_{1y}^e} & \frac{\partial l_{34}^e}{\partial u_{1y}^e} \\ \frac{\partial l_{12}^e}{\partial u_{1z}^e} & \frac{\partial l_{13}^e}{\partial u_{1z}^e} & \frac{\partial l_{14}^e}{\partial u_{1z}^e} & \frac{\partial l_{23}^e}{\partial u_{1z}^e} & \frac{\partial l_{24}^e}{\partial u_{1z}^e} & \frac{\partial l_{34}^e}{\partial u_{1z}^e} \\ \frac{\partial l_{12}^e}{\partial u_{2x}^e} & \frac{\partial l_{13}^e}{\partial u_{2x}^e} & \frac{\partial l_{14}^e}{\partial u_{2x}^e} & \frac{\partial l_{23}^e}{\partial u_{2x}^e} & \frac{\partial l_{24}^e}{\partial u_{2x}^e} & \frac{\partial l_{34}^e}{\partial u_{2x}^e} \\ \frac{\partial l_{12}^e}{\partial u_{2y}^e} & \frac{\partial l_{13}^e}{\partial u_{2y}^e} & \frac{\partial l_{14}^e}{\partial u_{2y}^e} & \frac{\partial l_{23}^e}{\partial u_{2y}^e} & \frac{\partial l_{24}^e}{\partial u_{2y}^e} & \frac{\partial l_{34}^e}{\partial u_{2y}^e} \\ \frac{\partial l_{12}^e}{\partial u_{2z}^e} & \frac{\partial l_{13}^e}{\partial u_{2z}^e} & \frac{\partial l_{14}^e}{\partial u_{2z}^e} & \frac{\partial l_{23}^e}{\partial u_{2z}^e} & \frac{\partial l_{24}^e}{\partial u_{2z}^e} & \frac{\partial l_{34}^e}{\partial u_{2z}^e} \\ \frac{\partial l_{12}^e}{\partial u_{3x}^e} & \frac{\partial l_{13}^e}{\partial u_{3x}^e} & \frac{\partial l_{14}^e}{\partial u_{3x}^e} & \frac{\partial l_{23}^e}{\partial u_{3x}^e} & \frac{\partial l_{24}^e}{\partial u_{3x}^e} & \frac{\partial l_{34}^e}{\partial u_{3x}^e} \\ \frac{\partial l_{12}^e}{\partial u_{3y}^e} & \frac{\partial l_{13}^e}{\partial u_{3y}^e} & \frac{\partial l_{14}^e}{\partial u_{3y}^e} & \frac{\partial l_{23}^e}{\partial u_{3y}^e} & \frac{\partial l_{24}^e}{\partial u_{3y}^e} & \frac{\partial l_{34}^e}{\partial u_{3y}^e} \\ \frac{\partial l_{12}^e}{\partial u_{3z}^e} & \frac{\partial l_{13}^e}{\partial u_{3z}^e} & \frac{\partial l_{14}^e}{\partial u_{3z}^e} & \frac{\partial l_{23}^e}{\partial u_{3z}^e} & \frac{\partial l_{24}^e}{\partial u_{3z}^e} & \frac{\partial l_{34}^e}{\partial u_{3z}^e} \\ \frac{\partial l_{12}^e}{\partial u_{4x}^e} & \frac{\partial l_{13}^e}{\partial u_{4x}^e} & \frac{\partial l_{14}^e}{\partial u_{4x}^e} & \frac{\partial l_{23}^e}{\partial u_{4x}^e} & \frac{\partial l_{24}^e}{\partial u_{4x}^e} & \frac{\partial l_{34}^e}{\partial u_{4x}^e} \\ \frac{\partial l_{12}^e}{\partial u_{4y}^e} & \frac{\partial l_{13}^e}{\partial u_{4y}^e} & \frac{\partial l_{14}^e}{\partial u_{4y}^e} & \frac{\partial l_{23}^e}{\partial u_{4y}^e} & \frac{\partial l_{24}^e}{\partial u_{4y}^e} & \frac{\partial l_{34}^e}{\partial u_{4y}^e} \\ \frac{\partial l_{12}^e}{\partial u_{4z}^e} & \frac{\partial l_{13}^e}{\partial u_{4z}^e} & \frac{\partial l_{14}^e}{\partial u_{4z}^e} & \frac{\partial l_{23}^e}{\partial u_{4z}^e} & \frac{\partial l_{24}^e}{\partial u_{4z}^e} & \frac{\partial l_{34}^e}{\partial u_{4z}^e} \end{bmatrix}$$

$$= \begin{bmatrix} \cos \phi_x^{12} & \cos \phi_x^{13} & \cos \phi_x^{14} & 0 & 0 & 0 \\ \cos \phi_y^{12} & \cos \phi_y^{13} & \cos \phi_y^{14} & 0 & 0 & 0 \\ \cos \phi_z^{12} & \cos \phi_z^{13} & \cos \phi_z^{14} & 0 & 0 & 0 \\ -\cos \phi_x^{12} & 0 & 0 & \cos \phi_x^{23} & \cos \phi_x^{24} & 0 \\ -\cos \phi_y^{12} & 0 & 0 & \cos \phi_y^{23} & \cos \phi_y^{24} & 0 \\ -\cos \phi_z^{12} & 0 & 0 & \cos \phi_z^{23} & \cos \phi_z^{24} & 0 \\ 0 & -\cos \phi_x^{13} & 0 & -\cos \phi_x^{23} & 0 & \cos \phi_x^{34} \\ 0 & -\cos \phi_y^{13} & 0 & -\cos \phi_y^{23} & 0 & \cos \phi_y^{34} \\ 0 & -\cos \phi_z^{13} & 0 & -\cos \phi_z^{23} & 0 & \cos \phi_z^{34} \\ 0 & 0 & -\cos \phi_x^{14} & 0 & -\cos \phi_x^{24} & -\cos \phi_x^{34} \\ 0 & 0 & -\cos \phi_y^{14} & 0 & -\cos \phi_y^{24} & -\cos \phi_y^{34} \\ 0 & 0 & -\cos \phi_z^{14} & 0 & -\cos \phi_z^{24} & -\cos \phi_z^{34} \end{bmatrix} \quad (21)$$

where $\cos \phi_{\alpha}^{ij}$ denotes angle made by the edge formed by node i and j with $\alpha \in \{x, y, z\}$ axis.

4.2. Full expression of A_2

$$\begin{aligned} A_2 &= \left[\frac{\partial \epsilon_c^e}{\partial l_d^e} \right]^T = \left[\frac{\partial \mathbf{T}^{-1} \epsilon_d^e}{\partial l_d^e} \right]^T = \left[\frac{\partial \epsilon_d^e}{\partial l_d^e} \right]^T \mathbf{T}^{-T} \\ &= \left[\frac{\partial \epsilon_{12}^e}{\partial l_d^e} \quad \frac{\partial \epsilon_{13}^e}{\partial l_d^e} \quad \frac{\partial \epsilon_{14}^e}{\partial l_d^e} \quad \frac{\partial \epsilon_{23}^e}{\partial l_d^e} \quad \frac{\partial \epsilon_{24}^e}{\partial l_d^e} \quad \frac{\partial \epsilon_{34}^e}{\partial l_d^e} \right]^T \mathbf{T}^{-T} \\ &= \begin{bmatrix} \frac{1}{L_{12}^e} & 0 & 0 & 0 & 0 & 0 \\ 0 & \frac{1}{L_{13}^e} & 0 & 0 & 0 & 0 \\ 0 & 0 & \frac{1}{L_{14}^e} & 0 & 0 & 0 \\ 0 & 0 & 0 & \frac{1}{L_{23}^e} & 0 & 0 \\ 0 & 0 & 0 & 0 & \frac{1}{L_{24}^e} & 0 \\ 0 & 0 & 0 & 0 & 0 & \frac{1}{L_{34}^e} \end{bmatrix} \begin{bmatrix} \frac{\partial l_{12}^e}{\partial l_d^e} & \frac{\partial l_{12}^e}{\partial l_d^e} & \frac{\partial l_{12}^e}{\partial l_d^e} & \frac{\partial l_{12}^e}{\partial l_d^e} & \frac{\partial l_{12}^e}{\partial l_d^e} & \frac{\partial l_{12}^e}{\partial l_d^e} \\ \frac{\partial l_{13}^e}{\partial l_d^e} & \frac{\partial l_{13}^e}{\partial l_d^e} & \frac{\partial l_{13}^e}{\partial l_d^e} & \frac{\partial l_{13}^e}{\partial l_d^e} & \frac{\partial l_{13}^e}{\partial l_d^e} & \frac{\partial l_{13}^e}{\partial l_d^e} \\ \frac{\partial l_{14}^e}{\partial l_d^e} & \frac{\partial l_{14}^e}{\partial l_d^e} & \frac{\partial l_{14}^e}{\partial l_d^e} & \frac{\partial l_{14}^e}{\partial l_d^e} & \frac{\partial l_{14}^e}{\partial l_d^e} & \frac{\partial l_{14}^e}{\partial l_d^e} \\ \frac{\partial l_{23}^e}{\partial l_d^e} & \frac{\partial l_{23}^e}{\partial l_d^e} & \frac{\partial l_{23}^e}{\partial l_d^e} & \frac{\partial l_{23}^e}{\partial l_d^e} & \frac{\partial l_{23}^e}{\partial l_d^e} & \frac{\partial l_{23}^e}{\partial l_d^e} \\ \frac{\partial l_{24}^e}{\partial l_d^e} & \frac{\partial l_{24}^e}{\partial l_d^e} & \frac{\partial l_{24}^e}{\partial l_d^e} & \frac{\partial l_{24}^e}{\partial l_d^e} & \frac{\partial l_{24}^e}{\partial l_d^e} & \frac{\partial l_{24}^e}{\partial l_d^e} \\ \frac{\partial l_{34}^e}{\partial l_d^e} & \frac{\partial l_{34}^e}{\partial l_d^e} & \frac{\partial l_{34}^e}{\partial l_d^e} & \frac{\partial l_{34}^e}{\partial l_d^e} & \frac{\partial l_{34}^e}{\partial l_d^e} & \frac{\partial l_{34}^e}{\partial l_d^e} \end{bmatrix}^T \mathbf{T}^{-T} \\ &= \begin{bmatrix} \frac{1}{L_{12}^e} & 0 & 0 & 0 & 0 & 0 \\ 0 & \frac{1}{L_{13}^e} & 0 & 0 & 0 & 0 \\ 0 & 0 & \frac{1}{L_{14}^e} & 0 & 0 & 0 \\ 0 & 0 & 0 & \frac{1}{L_{23}^e} & 0 & 0 \\ 0 & 0 & 0 & 0 & \frac{1}{L_{24}^e} & 0 \\ 0 & 0 & 0 & 0 & 0 & \frac{1}{L_{34}^e} \end{bmatrix} \begin{bmatrix} 1 & 0 & 0 & 0 & 0 & 0 \\ 0 & 1 & 0 & 0 & 0 & 0 \\ 0 & 0 & 1 & 0 & 0 & 0 \\ 0 & 0 & 0 & 1 & 0 & 0 \\ 0 & 0 & 0 & 0 & 1 & 0 \\ 0 & 0 & 0 & 0 & 0 & 1 \end{bmatrix} \mathbf{T}^{-T} \\ &= \begin{bmatrix} \frac{1}{L_{12}^e} & 0 & 0 & 0 & 0 & 0 \\ 0 & \frac{1}{L_{13}^e} & 0 & 0 & 0 & 0 \\ 0 & 0 & \frac{1}{L_{14}^e} & 0 & 0 & 0 \\ 0 & 0 & 0 & \frac{1}{L_{23}^e} & 0 & 0 \\ 0 & 0 & 0 & 0 & \frac{1}{L_{24}^e} & 0 \\ 0 & 0 & 0 & 0 & 0 & \frac{1}{L_{34}^e} \end{bmatrix} \mathbf{T}^{-T} \end{aligned} \quad (22)$$

5. Difference Between Graph-Based FEM and Mass-Spring Model

It can be tempting to assume that our model is similar to mass-spring or peridynamics-based fracture model [LBC* 15], reformulated as FEM. However, there exist two crucial differences.

First, in peridynamics or mass-spring model the total energy density of an element with n_e number of nodes, can be formulated as

$$\Psi^e = \sum_{i=1}^{n_e} \sum_{i>j}^{n_e} \Psi_{ij}^e \quad (23)$$

That is, the strain energy density is just the sum of the strain energies along each edge without any cross dependence. But in the case of

graph-based FEM method, strain energy density depends on the distance between all the edges of the element which is not just a simple sum. This is also observed by [RS15].

Second, in the case of peridynamics, force at any point depends on points far away from it. Therefore it is a completely non-local dynamics, whereas, in graph-based FEM, force values of an element are derived locally from the same element stresses.

6. Failed Approaches For Reformulating Energy Density for Non-linear Graph-based FEM

6.1. First Approach - Optimization based

Plugging in the optimized strain tensor $\hat{\mathbf{C}} = \mathcal{T} \cdot [Q \otimes Q]^\dagger \cdot Q$ from Theorem 2.1 to the set of invariants and subsequently calculating elastic strain energy density using these updated invariants, may seem a promising direction for internal force and tangent stiffness matrix calculation after fracture. However, the major problem of the optimization procedure is that it produces odd values of $\hat{\mathbf{C}}$ which are not practically consistent with the fractured state of the element. These odd values in turn make the movement of disjoint fractured segments erratic and render the simulation unstable. In Figure 1 we show the results for this approach on a 2D bar on which external force applied is applied at one end while keeping the other end hinged. Thus this approach does not work. Moreover, we notice that performing the optimization operation in every time step is extremely time consuming.

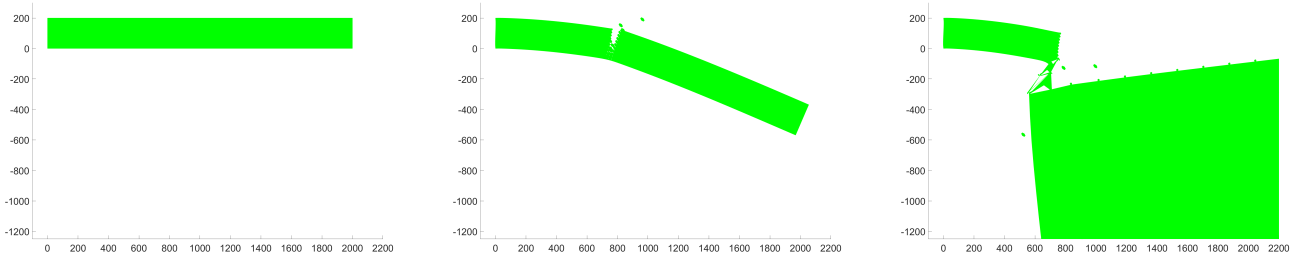


Figure 1: First failed approach for simulating fracture on a 2D bar.

6.2. Second Approach - Coordinate transform

While using non-linear hyper-elastic strain energy density, the internal force vector, \mathbf{f}_e^{int} and tangent stiffness matrix, \mathbf{k}_e can be defined as

$$\begin{aligned} \mathbf{f}_e^{int} &= \int_{\Delta_e} \frac{\partial \Psi^e}{\partial \mathbf{u}} d\xi = \int_{\Delta_e} \left[\frac{\partial \Psi^e}{\partial \mathbf{F}} \right] \left[\frac{\partial \mathbf{F}}{\partial \mathbf{u}} \right] d\xi \\ &= V_e \mathbf{P}(\mathbf{F}) \left[\frac{\partial \mathbf{F}}{\partial \mathbf{u}} \right] \end{aligned} \quad (24)$$

$$\begin{aligned} \mathbf{k}_e &= \int_{\Delta_e} \frac{\partial \mathbf{f}_e^{int}}{\partial \mathbf{u}} d\xi = \int_{\Delta_e} \left[\frac{\partial \mathbf{f}_e^{int}}{\partial \mathbf{F}} \right] \left[\frac{\partial \mathbf{F}}{\partial \mathbf{u}} \right] d\xi \\ &= V_e \left[\frac{\partial \mathbf{F}}{\partial \mathbf{u}} \right]^T \left[\frac{\partial \mathbf{P}}{\partial \mathbf{F}} \right] \left[\frac{\partial \mathbf{F}}{\partial \mathbf{u}} \right] \end{aligned} \quad (25)$$

Now one intuitive way to incorporate fractured stress value to Equation 24 is to transform the Cartesian component of Piola-Kirchhoff stress tensor, $\mathbf{P}(\mathbf{F})$ to the normal stress tensor along the edges, then apply zero stress values to the edges that are broken using fracture threshold criteria and finally transform them back to the Cartesian space again.

$$[\sigma_{c_{frac}}^e]^T = \mathbf{T}^{-1} \zeta \mathbf{T} [\sigma_c^e]^T \quad (26)$$

Finally, plugging in the values of $\sigma_{c_{frac}}^e$ in Equation 24 it may be assumed that we get back the fractured internal forces. Similarly, the same procedure can be followed for tangent stiffness matrix, \mathbf{k}_e in Equation 25.

However, following this line of thought does not work and it blows up the simulation as shown in Figure 2. The reason for this can be seen from the derivation of internal force and tangent stiffness matrix for the linear case of graph-based FEM. As shown in Equation 38, the matrix \mathbf{B} is denoted by $\mathbf{A}_2^T \mathbf{A}_1^T$ in linear case. However, for non-linear case in Equation 24 and Equation 25 the matrix \mathbf{B} is $\frac{\partial \mathbf{F}}{\partial \mathbf{u}}$ which is not same as linear case. Thus if we follow this approach, we have to derive the matrix \mathbf{B} from the fractured hyper-elastic strain energy density equation

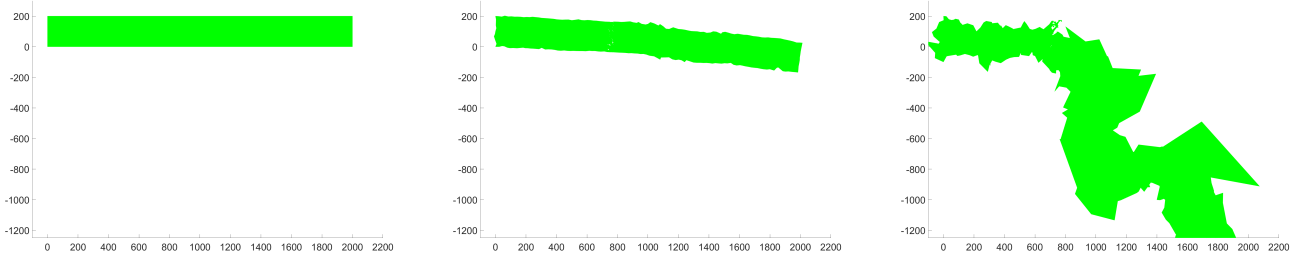


Figure 2: Second failed approach for simulating fracture on a 2D bar.

similar to the linear case. However, for non-linear case the hyper-elastic strain energy density is not a simple function of multiplication of stress and strain $\Psi^e = \frac{1}{2} \sigma_c^e \cdot \epsilon_c^e$ but rather depends on lower order invariants e.g., $\{I_C, II_C, III_C\}$ of Cauchy-Green deformation tensor \mathbf{C} . We did not find a suitable way of rewriting the invariants $\{I_C, II_C, III_C\}$ in damaged state due to the problematic pseudo-inverse operation as discussed previously. Thus, we are not able to derive \mathbf{B} and damaged stress $\sigma_{c_{frac}}^e$ using edge-based criteria similar to the linear case. Moreover, note that in linear case the damaged internal elastic force $\mathbf{f}_{e_{frac}}^{int}$ (Equation 19) and tangent stiffness matrix $\mathbf{k}_{e_{frac}}$ (Equation 20) depend on the damage matrix ζ quadratically. If we just plug in damaged stress $\sigma_{c_{frac}}^e$ from Equation 26 into Equation 24 and Equation 25, the dependence on ζ will be only linear, which is incorrect.

7. Linearization of Hyperelastic Strain Energy Density

7.1. Saint–Venant Kirchhoff energy density

The expression for StVK energy density is as follows.

$$\Psi_{stvk} = \frac{\lambda}{8} (I_C - 3)^2 + \frac{\mu}{4} (II_C - 2I_C + 3) \quad (27)$$

The energy expression can be rewritten [SSB13] in terms of Lagrangian finite strain tensor $\mathbf{E} = 1/2 (\mathbf{F}^T \mathbf{F} - \mathbf{I})$ as

$$\Psi_{stvk} = \frac{\lambda}{2} (\text{trace}(\mathbf{E}))^2 + \mu \mathbf{E} : \mathbf{E} \quad (28)$$

The PK1 stress for the StVK energy density is

$$\mathbf{P}(\mathbf{F}) = 2\mu \mathbf{E} + \lambda \text{trace}(\mathbf{E}) \mathbf{I} \quad (29)$$

Replacing Lagrangian finite strain tensor, \mathbf{E} with infinitesimal linearized strain tensor $\epsilon = 1/2(\mathbf{F} + \mathbf{F}^T) - \mathbf{I}$ and PK1 stress with linearized stress, σ , we get

$$\sigma = 2\mu \epsilon + \lambda \text{trace}(\epsilon) \mathbf{I} \quad (30)$$

Thus for StVK energy density $\mu = \mu_{\text{Lamé}}$ and $\lambda = \lambda_{\text{Lamé}}$.

7.2. Neo-Hookean energy density

The Neo-Hookean energy density can be expressed as

$$\Psi_{neo} = \frac{\mu}{2} (I_C - 3) + \frac{\lambda}{2} (J - \alpha)^2 - \frac{\mu}{2} \log(I_C + 1) \quad (31)$$

where $\alpha = 1 + \frac{\mu}{\lambda} - \frac{\mu}{4\lambda}$.

The PK1 stress for the Neo-Hookean energy density is

$$\mathbf{P}(\mathbf{F}) = \mu \left(1 - \frac{1}{I_C + 1} \right) \mathbf{F} + \lambda (J - \alpha) \frac{\partial J}{\partial \mathbf{F}} \quad (32)$$

Like before replacing PK1 stress with linearized stress, σ ,

$$\sigma = \mu \left(1 - \frac{1}{I_C + 1} \right) \mathbf{F} + \lambda (J - \alpha) \frac{\partial J}{\partial \mathbf{F}}$$

$$\begin{aligned}
&= \mu \left(1 - \frac{1}{I_C + 1} \right) \mathbf{F} + \lambda \left(J - 1 - \frac{\mu}{\lambda} + \frac{\mu}{4\lambda} \right) J \mathbf{F}^{-T}, \quad \text{using } \frac{\partial J}{\partial \mathbf{F}} = J \mathbf{F}^{-T} \\
&= \mu \mathbf{F} - \frac{\mu \mathbf{F}}{I_C + 1} + \left(\lambda \text{trace}(\boldsymbol{\varepsilon}) - \frac{3\mu}{4} \right) (1 + \text{trace}(\boldsymbol{\varepsilon})) \mathbf{F}^{-T}, \quad \text{using } J \approx 1 + \text{trace}(\boldsymbol{\varepsilon}) \\
&= \mu \left(\mathbf{F} - \frac{3}{4} \mathbf{F}^{-T} \right) - \frac{\mu \mathbf{F}}{I_C + 1} + \left(\lambda - \frac{3\mu}{4} \right) \text{trace}(\boldsymbol{\varepsilon}) \mathbf{F}^{-T}, \quad \text{ignoring } \text{trace}(\boldsymbol{\varepsilon})^2 \\
&= \mu \left(\mathbf{F} \mathbf{F}^T - \frac{3}{4} \mathbf{I} \right) \mathbf{F}^{-T} - \frac{\mu \mathbf{F}}{I_C + 1} + \left(\lambda - \frac{3\mu}{4} \right) \text{trace}(\boldsymbol{\varepsilon}) \mathbf{F}^{-T} \\
&= \mu \left(\mathbf{I} + 2\boldsymbol{\varepsilon} - \frac{3}{4} \mathbf{I} \right) \mathbf{F}^{-T} - \frac{\mu \mathbf{F}}{I_C + 1} + \left(\lambda - \frac{3\mu}{4} \right) \text{trace}(\boldsymbol{\varepsilon}) \mathbf{F}^{-T}, \quad \text{using } \mathbf{F} \mathbf{F}^T \approx \mathbf{I} + 2\boldsymbol{\varepsilon} \\
&= 2\mu \boldsymbol{\varepsilon} \mathbf{F}^{-T} + \mu \left(\frac{\mathbf{I}}{4} - \frac{\mathbf{F} \mathbf{F}^T}{I_C + 1} \right) \mathbf{F}^{-T} + \left(\lambda - \frac{3\mu}{4} \right) \text{trace}(\boldsymbol{\varepsilon}) \mathbf{F}^{-T} \\
&= 2\mu \boldsymbol{\varepsilon} + \mu \left(\frac{\mathbf{I}}{4} - \frac{\mathbf{I} + 2\boldsymbol{\varepsilon}}{I_C + 1} \right) + \left(\lambda - \frac{3\mu}{4} \right) \text{trace}(\boldsymbol{\varepsilon}) \mathbf{I}, \quad \text{using } \mathbf{F}^{-T} \approx \mathbf{I} \text{ and } \mathbf{F} \mathbf{F}^T \approx \mathbf{I} + 2\boldsymbol{\varepsilon} \\
&= 2\mu \boldsymbol{\varepsilon} + \mu \left(\frac{\mathbf{I}}{4} - \frac{\mathbf{I} + 2\boldsymbol{\varepsilon}}{4 + 2\text{trace}(\boldsymbol{\varepsilon})} \right) + \left(\lambda - \frac{3\mu}{4} \right) \text{trace}(\boldsymbol{\varepsilon}) \mathbf{I}, \quad \text{using } I_C \approx 3 + 2\text{trace}(\boldsymbol{\varepsilon}) \\
&= 2\mu \boldsymbol{\varepsilon} + \mu \left(\frac{\mathbf{I}}{4} - \frac{1}{4} (\mathbf{I} + 2\boldsymbol{\varepsilon}) \left(1 - \frac{\text{trace}(\boldsymbol{\varepsilon})}{2} \right) \right) + \left(\lambda - \frac{3\mu}{4} \right) \text{trace}(\boldsymbol{\varepsilon}) \mathbf{I}, \quad \text{using } \left(1 + \frac{\text{trace}(\boldsymbol{\varepsilon})}{2} \right)^{-1} \approx \left(1 - \frac{\text{trace}(\boldsymbol{\varepsilon})}{2} \right) \\
&= 2\mu \boldsymbol{\varepsilon} - \frac{\mu \boldsymbol{\varepsilon}}{2} + \frac{\mu \text{trace}(\boldsymbol{\varepsilon}) \mathbf{I}}{8} + \frac{\mu \text{trace}(\boldsymbol{\varepsilon}) \boldsymbol{\varepsilon}}{4} + \left(\lambda - \frac{3\mu}{4} \right) \text{trace}(\boldsymbol{\varepsilon}) \mathbf{I} \\
&= \frac{3}{2} \mu \boldsymbol{\varepsilon} \left(1 + \frac{\text{trace}(\boldsymbol{\varepsilon})}{6} \right) + \left(\lambda - \frac{5\mu}{8} \right) \text{trace}(\boldsymbol{\varepsilon}) \mathbf{I} \\
&= \frac{3}{2} \mu \boldsymbol{\varepsilon} + \left(\lambda - \frac{5\mu}{8} \right) \text{trace}(\boldsymbol{\varepsilon}) \mathbf{I} \quad \text{using } \left(1 + \frac{\text{trace}(\boldsymbol{\varepsilon})}{6} \right) \approx 1
\end{aligned} \tag{33}$$

So comparing them with $2\mu_{\text{Lamé}} = \frac{3}{2}\mu \implies \mu = \frac{4}{3}\mu_{\text{Lamé}}$ and $\lambda_{\text{Lamé}} = \lambda - \frac{5}{8}\mu \implies \lambda = \lambda_{\text{Lamé}} + \frac{5}{8}\mu \implies \lambda = \lambda_{\text{Lamé}} + \frac{5}{6}\mu_{\text{Lamé}}$. The approximations we have used can be found in [Wik22].

References

- [LBC*15] LEVINE J. A., BARGTEIL A. W., CORSI C., TESSENDORF J., GEIST R.: A peridynamic perspective on spring-mass fracture. In *Proceedings of the ACM SIGGRAPH/Eurographics Symposium on Computer Animation* (Goslar, DEU, 2015), SCA '14, Eurographics Association, p. 47–55. [5](#)
- [MG04] MÜLLER M., GROSS M.: Interactive virtual materials. In *Proceedings of Graphics Interface* (Waterloo, CAN, 2004), Canadian Human-Computer Communications Society, p. 239–246. [3](#)
- [RS15] REDDY J., SRINIVASA A.: On the force–displacement characteristics of finite elements for elasticity and related problems. *Finite Elements in Analysis and Design* 104 (2015), 35 – 40. URL: <http://www.sciencedirect.com/science/article/pii/S0168874X15000682>, doi:<https://doi.org/10.1016/j.finel.2015.04.011>. [6](#)
- [SSB13] SIN F. S., SCHROEDER D., BARBIĆ J.: Vega: Non-linear fem deformable object simulator. *Computer Graphics Forum* 32, 1 (2013), 36–48. URL: <https://onlinelibrary.wiley.com/doi/abs/10.1111/j.1467-8659.2012.03230.x>, arXiv:<https://onlinelibrary.wiley.com/doi/pdf/10.1111/j.1467-8659.2012.03230.x>, doi:10.1111/j.1467-8659.2012.03230.x. [7](#)
- [Wik22] WIKIPEDIA: Neo-hookean solid, Nov. 2022. URL: https://en.wikipedia.org/wiki/Neo-Hookean_solid. [8](#)